Optimal Design of Azeotropic Batch Distillation

M. C. Mussati, P. A. Aguirre, J. Espinosa, and O. A. Iribarren
INGAR–Instituto de Desarrollo y Diseño (CONICET-UTN), Avellaneda 3657, (S3002GJC) Santa Fe, Argentina

DOI 10.1002/aic.10696
Published online October 10, 2005 in Wiley InterScience (www.interscience.wiley.com).

This study explores integrating models with different degrees of detail for optimizing azeotropic batch distillation systems. A detailed dynamic model is used from outside the optimization program both to verify feasibility of the design and to update the parameters needed by the optimization model. The updated parameters are the constant relative volatilities between pseudo-components, used in a binary Fenske–Underwood–Gilliland-type model. The approach was used to optimize the design of a batch process for the recovery of spent isopropyl alcohol, which works cyclically to separate the excess water, satisfying an environmentally acceptable specification, and using cyclohexane as entrainer, which in turn is recovered in the same process and recycled. The approach permitted optimizing the batch sizes, number of separation stages, the reflux ratios of a piecewise constant multilevel reflux policy, the extent of each separation, and the size of the intermediate cuts to be recycled, with affordable computation and problem setup times. © 2005 American Institute of Chemical Engineers *AIChE J,* 52: 968–985, 2006
Keywords: batch process design, azeotropic batch distillation, process optimization model

Introduction

Batch distillation plays an important role in the specialty and fine chemicals industries in the purification of liquid products and recovery of spent solvents, which usually form multicomponent azeotropic mixtures.

In designing such a system, the first problem to solve is the synthesis of a processing strategy, for which conceptual design approaches provide insight into the problem by assessing its bounds. Bernot et al.[1] synthesized batch distillation sequences for azeotropic mixtures with the aid of residue curve maps. Their analysis included both batch rectifiers and strippers in solving reaction–separation synthesis problems. Azeotropes produced are either broken by using an appropriate entrainer, recycled back to the next batch, or recycled back to the reactor.

In this line there are several other contributions. Ahmad and Barton[2] solved the sequencing problem of reactors and distillation columns to minimize the amount of waste produced by the process. Based on their method to find "batch" distillation regions, they determined the best composition and amount of solvents fed to the reactors and the best recycling policy for the column products. Safrit and Westerberg[3] determined the network of all possible sequences based on determination of "batch" distillation regions and included batch rectifiers, batch strippers, middle vessel columns, and extractive middle vessel columns into their analysis. Rodriguez-Donis et al.[4] assessed feasibility using simplified models for the case of heterogeneous batch distillations emphasizing process flexibility through reflux policy. All these contributions use the assumption of total reflux/reboil ratio and infinite number of trays and include information about maximum feasible separation, taking into account distillation boundaries through determination of "batch" distillation regions.

Once the processing strategy has been defined, the decision among the various available column operations (such as rectifier, stripper, middle vessel, etc.) could be refined through more detailed models that allow optimization of the reflux policy as first proposed by Chiotti et al.[5,6] to select between rectifiers and strippers for ideal systems. These investigators used a simplified model to represent the performance of distillation tasks to determine the optimal constant reflux/reboil ratios and cut locations while allowing the recycling of intermediate cuts.

Correspondence concerning this article should be addressed to O. A. Iribarren at iribarr@ceride.gov.ar.

Bernot et al.[7] developed a conceptual model to estimate batch sizes, operating time, equipment sizes, utility loads, and costs for the batch distillation of nonideal and azeotropic systems. Their model is integrated only once as it decouples the variation of compositions from the variation of flows and the batch sizes using a dimensionless "warped" time, provided that the amount and purity of each cut are previously determined from feasibility studies. Finally, they proposed a variable reflux/reboil ratio policy because it leads to costs savings compared to the constant reflux policy and it is easier to compute.

Sundaram and Evans[8] first proposed a superstructure formulation for this kind of problems. They generated a superstructure embedding all possible combinations of conducting the desired separations with available batch rectifiers. By incorporating a short-cut method based on Fenske–Underwood–Gilliland (FUG) equations into the optimization framework as a black box, these authors circumscribed the optimal sequence, reflux ratio policy, and cut locations for ideal mixtures. As mentioned, all these works use simplified models for the distillation node.

On the other hand, several authors used rigorous models to optimize new column arrangements or operating policies, such as when analyzing total reflux columns[9] and a multivessel batch distillation–decanter hybrid structure.[10]

This brief background does not intend to be a complete literature review, but serves to illustrate the following point: selecting among processing alternatives or considering complex configurations in some cases poses a limitation on the degree of detail that can be used for the distillation model. All the more complex synthesis problems described above resort to simplified models. After solving the synthesis problem, however, the next step is designing the column as rigorously as possible, or as practical.

Whether rigorous distillation models can be used practically depends on whether the synthesized process needs to consider complex mass balances and scheduling constraints between different processing steps. If the different pieces of the process work simultaneously, the process can be represented as a unique large dynamic model. In this case a rigorous model could be used, with the process behaving as a unique batch separation block, such as the total reflux column[9] or the multivessel batch distillation–decanter hybrid structure.[10]

However, if the different separations of the processing network are performed at different units that work cyclically on batches produced by some other unit, or performed sequentially at the same unit but also in a cyclic operation, then the scheduling and mass balances among these separations may practically preclude the use of rigorous models.

These processing strategies can be represented as a network of single-step separations connected by material balance constraints, known as a *state task network* (STN),[11] which is equivalent to the process flow sheet of a continuous process. The performance of the STN depends on the value of process variables at the task nodes, such as reflux ratios and extent of separations. In general, the state task network includes the generation of sloppy cuts and a policy about how they are recycled for reprocessing, that is, the STN is equivalent to a complex, highly nested flow sheet of a continuous process.

Up to some complexity of the problem formulations, it is still practical to use detailed dynamic distillation models accounting for nonidealities in vapor–liquid equilibrium, as proposed by Mujtaba and Macchietto,[12] who optimized multicomponent batch rectifications through a multiperiod formulation. The same authors also solved a more complex problem, which includes multiple separation duties, that is, different multicomponent feeds to be processed by the same column, including setup times between batches when needed.[13]

The use of detailed distillation models starts to be a formidable task when considering the recycling of intermediate off cuts, storage of batches, and the scheduling of all the tasks, such as the feeding of a batch to the still from a storage tank through a heater, the discharge of a main cut from the still through a cooler to an end product storage tank, and so forth.

On the other hand, these kinds of problems are affordable in practice with simplified distillation models. For example, Bhatia and Biegler[14] optimized a process including reaction and distillation stages with the recycle of a cut from the column back to the reactor, by resorting to a simplified FUG model for the distillation tasks, previously developed by Logsdon et al.[15] In this way they were able to optimize the molar conversions at the reaction steps and the reflux ratios at the distillation steps, satisfying both the scheduling and mass balances constraints.

A practical approach that can be used to solve the batch distillation design step within a short problem setup time is to optimize the process with simplified models, and then design the column with a more rigorous model, to guarantee that it will be able to perform each of the separation tasks in the times assigned.

Alternatively, herein we propose the integration of models with different degrees of detail for optimizing the design of batch distillation systems, which renders a better solution without much more effort. We use a previously developed conceptual dynamic model based on pinch analysis for nonideal mixtures[16] from outside the optimization program both to verify feasibility of the design and to update the parameters of the optimization model, which is of a lower degree of detail. The updated parameters are the constant relative volatilities between pseudo-components, used inside a Fenske–Underwood–Gilliland-type model.

The approach is illustrated optimizing the design of a column for the recovery of spent isopropyl alcohol that works cyclically to recycle the off cuts, that is, without producing any waste cut, but the excess water with an environmentally acceptable specification.

The article is organized as follows. First, the process and the distillation models are briefly described and, following, the interaction between the rigorous distillation model and the process optimization model is explained. Afterward, the implementation of the process optimization model is described to appropriately represent the design problem; that is, the economic trade-offs and practical constraints such as the merging of small-size batches before reprocessing, the computation of start-up and changeover times, and the rounding of cycle times to figures that are compatible with working shifts. Then, the results of the design are presented and discussed and, finally, the conclusions of this work are drawn.

Process Description

The process objective is to recover water-diluted isopropyl alcohol (IPA), using cyclohexane (CH) to break the azeotrope between the alcohol and water (W). The feed composition,

Table 1. Feed, Product, and Working Period Specifications

Fresh Feed Composition		
IPA	0.868	mole fraction
Water	0.132	mole fraction
Product Specification, Production Target, and Effluent Limits		
Production rate	25	m^3 per week
IPA purity (product)	>0.99	mole fraction
IPA content in wastewater	<1.1	kg/m^3
Water in product	<0.0124	mole fraction
Cyclohexane in product	<0.0028	mole fraction
Working Period		
Weeks per year	52	
Days per week	5	
Hours per day	24	

product specifications, and production target are presented in Table 1.

The process synthesis step was done with conceptual design methodologies and is described in detail by Espinosa et al.[17] Briefly, a software tool that integrates all the algorithms necessary—to approach, from azeotrope prediction and determination of distillation regions, to the calculation of minimum reflux, minimum number of stages, and maximum feasible separation for each separation task—was used to assess different process alternatives.

The selected alternative is presented in Figure 1a and requires two distillation steps that are performed in the same batch rectifier at different periods of time and one decantation step. The process mass balances can be described following the diagram in Figure 1b. The feed to the process F together with a distillate cut D_2 that comes from separation S_2 and an organic phase cut (OP) that comes from the decantation step [*L–L* Sep (*LLS*)] are charged in the still of a batch rectifier. Both D_2 and OP come from the previous cycle. The still content changes its composition from M to B_1—IPA in specification—whereas the ternary azeotrope is removed as distillate by the rectifying column. D_1 represents the overall amount of distillate collected after separation task S_1 is completed. The separation S_1 provides an almost complete recovery of the alcohol contained in the feed F.

The decantation step (*LLS*) done after separation S_1 splits D_1 into a cyclohexane-rich phase OP and a water-rich aqueous phase AP. The organic phase supplies the cyclohexane necessary for separation S_1 in the next cycle, whereas the aqueous phase is driven to separation task S_2 to obtain a wastewater cut B_2 and a distillate cut D_2—mainly IPA–W at its azeotropic composition—which is recycled to separation task S_1 in the next cycle.

The STN corresponding to the process that implements a multilevel reflux policy for separation S_1 is presented in Figure 2. The *States* are batches, that is, an amount of material in [kg] or [kmol] represented with a circle with a number, to identify it in the associated mass balances data sheet presented in Table 2. The *Tasks* are unit operations that change the state of the batches, such as distillation tasks, heating, cooling, settling, and so forth, and have been represented using different icons for each unit operation. This makes the STN representation look different from the original work,[11] where rectangles are used to represent every task.

The *Equipment Diagram* is presented in Figure 3 and does not coincide with the STN (in continuous processes they do coincide) because (1) the single distillation column performs several tasks consecutively and (2) several vessels have been duplicated as a result of scheduling considerations.

The sequencing of tasks is represented in a Gantt chart as illustrated in Figure 4, which corresponds to separation S_1. This is the final result, after deciding that the plant will produce weekly 14 consecutive cycles of 8 h of IPA and 1 cycle of 8 h of residual water. This is explained in more detail later.

The process is based on adding an amount of organic phase (OP) rich in cyclohexane (CH) to the feed such that water (W) and CH are exactly in the proportion of the ternary heteroazeotrope CH–IPA–W and separating this azeotrope from pure IPA in three consecutive distillation tasks, each one performed at a different constant reflux ratio. A multilevel reflux policy was adopted because it allows energy savings. The azeotrope is split into an OP and an AP at the settler. Once a week the AP is processed to produce a batch of wastewater in specification and recover the organics.

The fresh feed is vaporized in a crystallizer and condensed again: this task recovers a crystalline medicinal product by separating it from the IPA stream. This train operates contin-

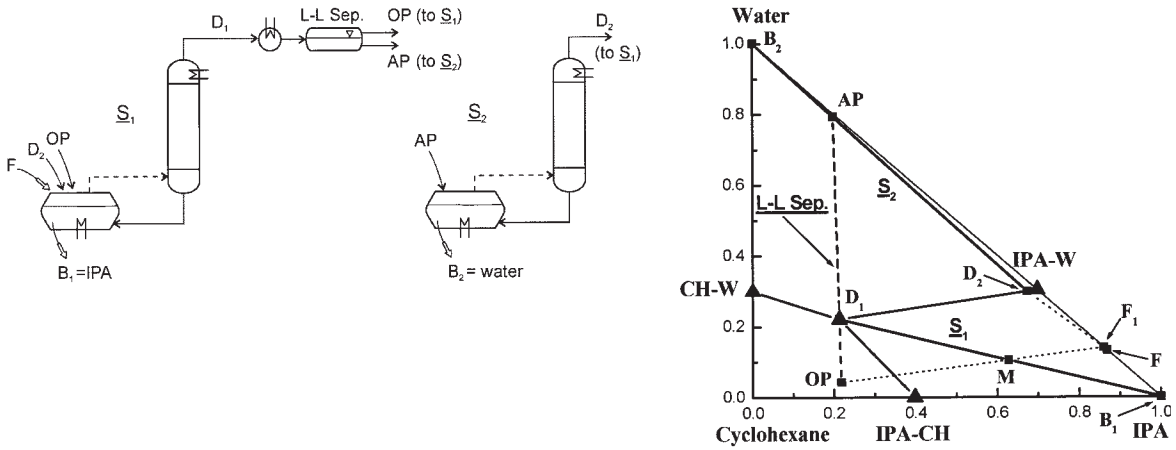

Figure 1. (a) Operation sequence synthesized in Espinosa et al.; [17](b) overall mass balances in the triangular diagram.

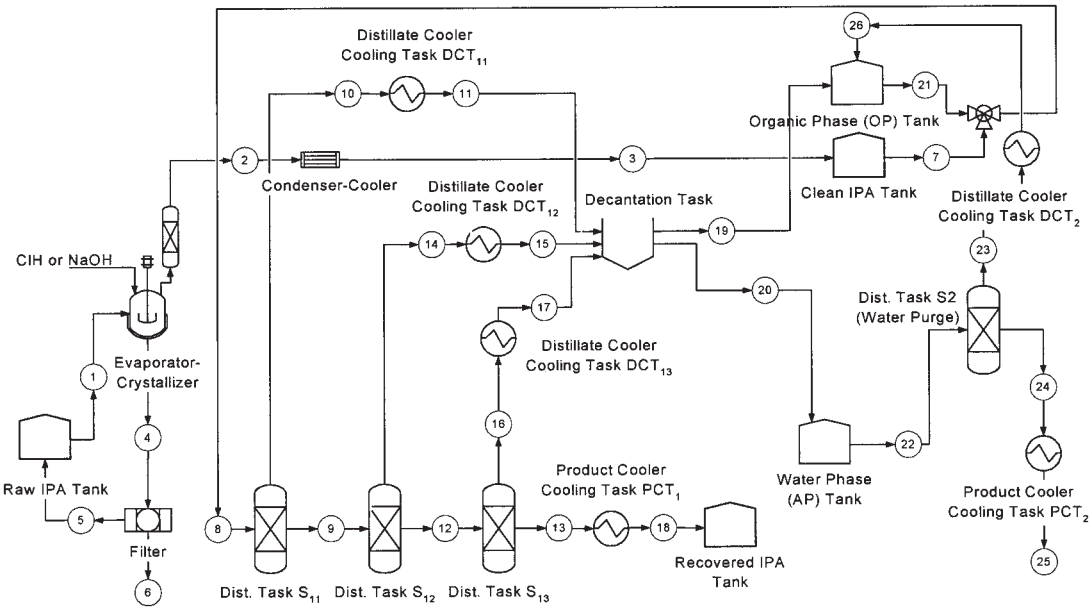

Figure 2. State-task network.

uously for IPA, with intermittent discharge of solids. IPA is alternatively stored in two holding tanks, as also occurs with the OP to provide waiting time in the tanks, enough for measuring their W and CH content. Therefore, the amount of OP that must be added to each IPA batch in the next shift can be calculated.

Because the column still has also been duplicated, the still is fed from the corresponding IPA and OP tanks and remains full until the next shift, when this batch will be processed. The reason for duplicating the still was to avoid column idle time: the column is not emptied between successive IPA processing tasks, nor are there idle times for charging and discharging the still.

The IPA processing shifts start cyclically with the column operating at total reflux with the compositions profile corresponding to the last instant of the previous shift: with IPA in specification in the bottom. The still corresponding to the last shift is disconnected and the new one is connected. Meanwhile the column bottom is fed directly to the boiler, skipping the stills.

The two first distillation tasks are conducted at reflux ratios such that the distillate produced is pure CH–IPA–W. To be sure that the liquid returning to the column also has this composition, the condenser was also duplicated, so the reflux ratio is controlled through a valve on the vapor exiting the column. The last distillation task is done at a larger reflux ratio to strip the IPA from CH and W.

The operation finishes when the temperature in the lower sections of the column corresponds to the IPA boiling point. The still is then disconnected. If the next shift is also of IPA processing, the holdups in the column and boiler remain there and the new still is connected. If it is the AP processing shift, the holdups are sent to an OP tank. In any case the IPA in the still is sent, through a cooler, to the product tank.

Distillation Models

Binary FUG model

Although the real system is ternary and posseses one ternary hetero-azeotrope CH–IPA–W plus three binary azeotropes: CH–W (heterogeneous), CH–IPA, and IPA–W (both homogeneous), it was shown[17] that feeding a mixture with the amounts of CH and W corresponding to the proportion of the ternary azeotrope allows conducting the separation along the residue line connecting the CH–IPA–W azeotrope composition and IPA, which were taken in the simplified model as pseudo-components to be separated by a binary distillation. By following these feeding and operating policies, the other azeotropic pseudo-components (CH–IPA or IPA–W) do not show up.

The simplified distillation model used in the optimization level was analytically derived for binary distillations by Salomone et al.[18] Using the binary Fenske equation for continuous distillation to relate the instantaneous top–bottom compositions of a batch column, they integrated the differential mass balances of a batch rectification to predict the minimum number of stages $N_{\min}$ needed by a hypothetical total reflux batch column to perform a given separation task:

$$N_{\min} = \frac{\ln \dfrac{\ln\left(\dfrac{x_{LD}-x_{LB}}{x_{LD}-x_{LF}}\dfrac{x_{LF}}{x_{LB}}\right)}{\ln\left(\dfrac{x_{LD}-x_{LB}}{x_{LD}-x_{LF}}\dfrac{1-x_{LF}}{1-x_{LB}}\right)}}{\ln \alpha_{LH}} \tag{1}$$

where x_{LD}, x_{LB}, and x_{LF} represent the mole fractions of the light-key component in the distillate, residue, and feed, respectively; and α_{LH} is the relative volatility between the light- and heavy-key components.

Bauerle and Sandall,[19] using the binary Underwood equation

Table 2. Mass Balances Data Sheet

Name	1	2	3	4
State	Liquid + Solids	Vapor	Liquid	Liquid + Solids
Temp., K	308.15	353.55	308.15	354.09
Pressure, kPa	100	100	100	100
Amount, kmol		26.7406	26.7406	
Amount, kg	~1604.8	1458.4607	1458.4607	~146.34
Volume, m	~2.068		1.9082	~0.186
Density, kg/m^3	775.85	1.88	764.31	786.77
Solids, mass fraction	~0.0283	0/0	0/0	~0.31
*IPA fraction	0.8434	0.9564/0.868	0.9564/0.868	0.5986
*Water fraction	0.1283	0.0436/0.132	0.0436/0.132	0.0914

Name	5	6	7	8
State	Liquid	Solid	Liquid	Liquid
Temp., K	354.09	354.09	308.15	341.18
Pressure, kPa	100	100	100	100
Amount, kmol	1.8504		26.7406	58.8542
Amount, kg	100.9235	~45.4158	1458.4607	3678.3875
Volume, m^3	0.1303	~0.056	1.9082	4.9868
Density, kg/m^3	774.71	817.29	764.31	737.63
*CH fraction	0/0	0	0/0	0.4235/0.3145
*IPA fraction	0.9564/0.868	0	0.9564/0.868	0.5411/0.5628
*Water fraction	0.0436/0.132	0	0.0436/0.132	0.035373/0.1227

Name	9	10	11	12
State	Liquid	Liquid	Liquid	Liquid
Temp., K	344.33	339.352	308.15	347.603
Pressure, kPa	100	100	100	100
Amount, kmol	37.7925	21.0617	21.06167	31.3780
Amount, kg	2323.0318	1355.4021	1355.4021	1910.1997
Volume, m^3	3.1961	1.8006	1.7277	2.6577
Density, kg/m^3	726.83	752.76	784.51	718.73
*CH fraction	0.2456/0.1794	0.7284/0.557	0.7284/0.557	0.1412/0.10215
*IPA fraction	0.7338/0.7506	0.2108/0.2257	0.21078/0.2257	0.847/0.858
*Water fraction	0.02052/0.07	0.06084/0.2173	0.06084/0.2173	0.01179/0.03985

Name	13	14	15	16
State	Liquid	Liquid	Liquid	Liquid
Temp., K	355.105	339.352	308.15	340.25
Pressure, kPa	100	100	100	100
Amount, kmol	23.3004	6.4145	6.4145	8.0776
Amount, kg	1400.7740	412.8193	412.8193	509.4387
Volume, m^3	1.9906	0.5484	0.52621	0.6860
Density, kg/m^3	703.69	752.78	784.52	742.63
*CH fraction	0.003920/0.0028	0.7288/0.5573	0.7288/0.5573	0.5187/0.3887
*IPA fraction	0.9957/0.9961	0.2103/0.2252	0.2103/0.2252	0.4379/0.4596
*Water fraction	0.000326/0.00109	0.06087/0.2175	0.06087/0.2175	0.04332/0.1517

Name	17	18	19	20
State	Liquid	Liquid	Liquid	Liquid
Temp., K	308.15	308.15	308.15	308.15
Pressure, kPa	100	100	100	100
Amount, kmol	8.0776	23.3004	28.2597	7.2941
Amount, kg	509.4387	1400.7740	2037.5512	240.1148
Volume, m^3	0.6554	1.8359	2.6317	0.2877
Density, kg/m^3	777.3	762.97	774.22	834.57
*CH fraction	0.5187/0.3887	0.003920/0.0028	0.75194/0.6442	0.08449/0.03305
*IPA fraction	0.4379/0.4596	0.9957/0.9961	0.2273/0.2727	0.5517/0.3022
*Water fraction	0.04332/0.1517	0.000326/0.00109	0.02076/0.0831	0.3638/0.6647

for continuous distillation to relate the instantaneous top–bottom compositions of a batch column, derived the expression for the minimum reflux $R_{\min}$ needed by a hypothetical batch column with infinite number of trays to perform a given separation task:

$$R_{\min} = \frac{\ln\left[\left(\frac{1 - x_{LF}}{1 - x_{LB}}\right)^{\alpha_{LH}} \frac{x_{LB}}{x_{LF}}\right]}{(\alpha_{LH} - 1)\ln\left(\frac{x_{LD} - x_{LF}}{x_{LD} - x_{LB}}\right)} - 1 \qquad (2)$$

Table 2. (Continued)

Name	1	2	3	4
Name	**21**	**22**	**23**	**24**
State	Liquid	Liquid	Liquid	Liquid
Temp., K	308.15	346.87	346.21	373.148
Pressure, kPa	100	100	100	100
Amount, kmol	28.2597	7.2941	3.7885	3.5056
Amount, kg	2037.5512	240.1148	176.9011	63.2128
Volume, m^3	2.6244	0.3018	0.2391	0.06669
Density, kg/m^3	776.38	795.56	739.89	947.92
*CH fraction	0.7010/0.5756	0.08449/0.03305	0.1146/0.0636	0.000187/0.00004
*IPA fraction	0.2689/0.3092	0.5517/0.3022	0.7485/0.5816	0.0011/0.00033
*Water fraction	0.03004/0.1152	0.36378/0.6647	0.1369/0.3548	0.9987/0.9996
Name	**25**	**26**		
State	Liquid	Liquid		
Temp., K	308.15	308.15		
Pressure, kPa	100	100		
Amount, kmol	3.5056	3.7885		
Amount, kg	63.2128	176.9011		
Volume, m^3	0.06322	0.2261		
Density, kg/m^3	999.8	782.23		
*CH fraction	0.000187/0.00004	0.1146/0.0636		
*IPA fraction	0.0011/0.00033	0.7485/0.5816		
*Water fraction	0.9987/0.9996	0.1369/0.3548		

*Mass Fraction/Mole Fraction

which is valid as long as both components distribute, with a pinch at the bottom of the column.

Actually, for a given reflux, the limiting condition for distribution occurs when the instantaneous bottom composition has an intermediate value x_{LI} such that the binary Underwood equation for continuous distillation predicts that the top composition is 1, that is,

$$R_{\min} = \frac{1}{(\alpha_{LH} - 1)x_{LI}} \tag{3}$$

For still compositions $> x_{LI}$ a pinch at the column top controls the separation and only the light component exits the

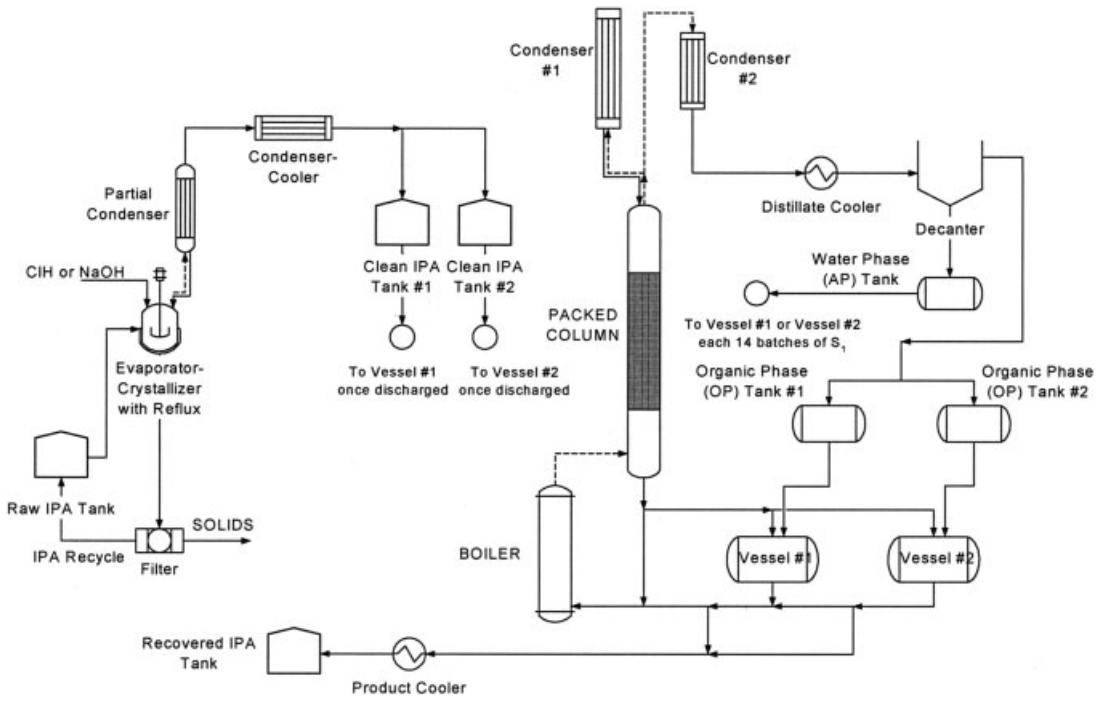

Figure 3. Equipment diagram.

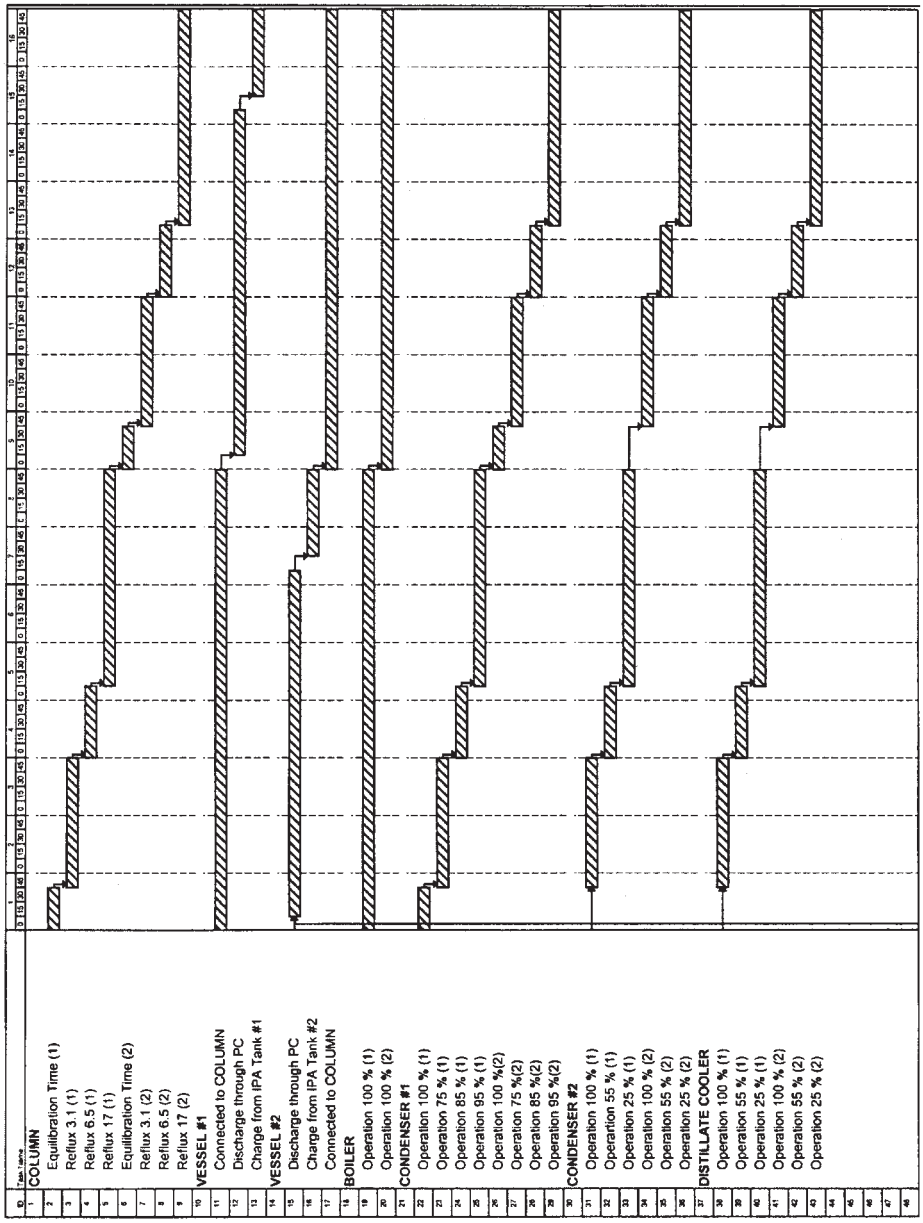

Figure 4. Gantt chart.

column, and for a distillation that goes through both zones Salomone et al. derived[18]

$$R_{\min} = \frac{\ln\left[\left(\frac{1 - x_{LI}}{1 - x_{LB}}\right)^{\alpha_{LH}} \frac{x_{LB}}{x_{LI}}\right]}{(\alpha_{LH} - 1)\ln\left(\frac{x_{LD} - x_{LF}}{x_{LD} - x_{LB}} \frac{1 - x_{LI}}{1 - x_{LF}}\right)} - 1 \qquad (4)$$

$$x_{LI} \leq x_{LF} \qquad x_{LI} \geq x_{LB}$$

which takes into account that for still compositions $> x_{LI}$ only the light component is taken as an overhead product, and for instantaneous still compositions $< x_{LI}$ the process is governed by Eq. 2. Equation 4 must be solved together with Eq. 3 to obtain x_{LI} and $R_{\min}$. Finally, $N_{\min}$ and $R_{\min}$ can be related to the actual number of stages N and reflux ratio R by using a Gilliland-like correlation that was constructed for batch distillation[18]:

$$\left(\frac{N - N_{\min}}{N + 1}\right) = 0.62\left[1 - \left(\frac{R - R_{\min}}{R + 1}\right)^{0.34}\right] \qquad (5)$$

In the implementation of this model three distillation tasks were adopted for the IPA recovery task. The two first distillation tasks occur above the respective x_{LI}, so only CH–IPA–W azeotrope is withdrawn from the column, whereas the third distillation task goes through both zones and implements Eqs. 3 and 4. When processing the AP, the pseudo-components present are the ternary azeotrope CH–IPA–W in only a slight amount, the binary azeotrope IPA–W and W; thus CH–IPA–W

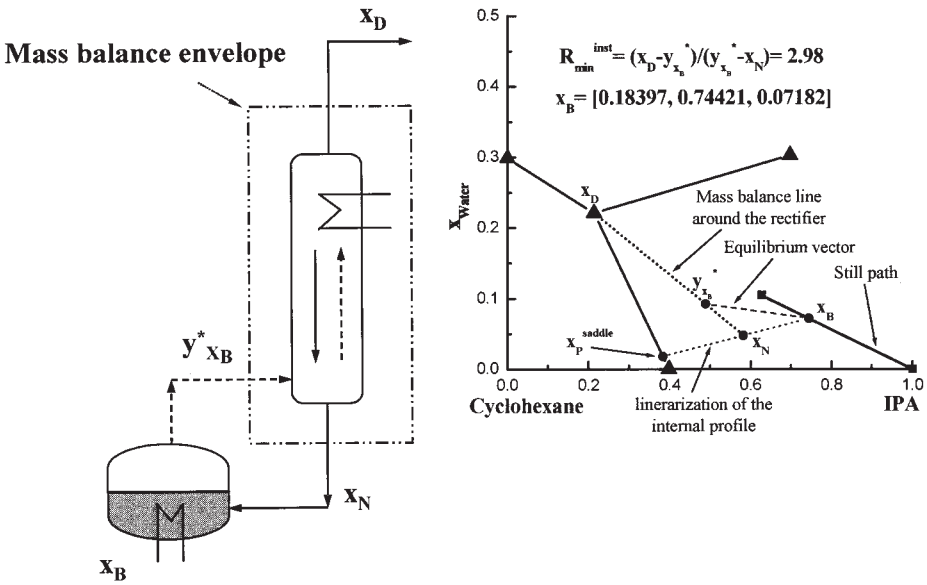

Figure 5. (a) Mass balance envelope; (b) minimum reflux ratio to reach a distillate with the composition of the ternary azeotrope from an instantaneous still composition x_B.

x_N represents the composition of the liquid stream in the stage immediately above the reboiler.

and IPA–W are grouped together to constitute the light component, assigning a relative volatility α between IPA–W and W. In this case, only one separation task (a single constant reflux ratio) was implemented.

Conceptual model

The conceptual dynamic model used outside the optimization program, proposed by Espinosa et al.,[17] allows evaluation of the separation power: that is, the minimum number of stages and minimum reflux needed for achieving a given purity requirement of key components.

To evaluate the minimum energy demand of a given separation, column performance at different reflux policies must be calculated. The basic assumptions are a batch rectifier having an infinite number of stages and quasi-stationary operation of the column. Therefore, the pinch theory can be applied. A material balance around the batch rectifier permits calculation of the process of batch distillation of a multicomponent mixture. Thus, recoveries of the components in the distillate as a function of the rectification advance are calculated through integration of the following differential–algebraic equation system:

$$\frac{d\sigma_{iD}}{d\eta} = \frac{x_{iD}}{x_{i0}} \tag{6}$$

$$x_{iB} = x_{i0}\frac{(1-\sigma_{iD})}{(1-\eta)} \tag{7}$$

where σ_{iD} is the fractional recovery of component i in the distillate, η is the rectification advance, x_{iD} is the mole fraction of component i in the distillate, x_{i0} is the initial mole fraction of component i in the still, and x_{iB} is the instantaneous mole fraction of component i in the still. All the other variables—such as recoveries of the components in the residue, distillate, and residue compositions, and top and residue temperatures—can be calculated as a function of component recoveries in the distillate and rectification advance as shown in Eq. 7 for x_B.

To integrate Eqs. 6 and 7 without resorting to stage-by-stage calculations, pinch theory is applied to estimate x_D from x_B as distillation proceeds for operation at constant reflux. Operation at constant distillate composition, on the other hand, requires determination of the instantaneous minimum reflux $R_{\min}^{inst}$ for instantaneous still composition x_B.

As mentioned earlier, operation at constant reflux requires determination of instantaneous distillate composition x_D corresponding to instantaneous still composition x_B from a mass balance around the rectifier (Figure 5a). The key to the method is the estimation of the composition of the liquid leaving the column bottom, x_N (Figures 5a and 5b). This composition is located on the linear approximation of the internal profile in the neighborhood of x_B, which in turn can be obtained by solving an eigenvalue problem of the Jacobian of the equilibrium at x_B.[16] Depending on the value of the reflux ratio three pinch topologies can appear:

(1) *Low reflux ratio*: a pinch at the column bottom controls the separation with $x_N = x_B$. The instantaneous distillate composition, calculated from the mass balance around the rectifier, belongs to the line given by x_B and its vapor in equilibrium y^*_{xB}.

(2) *Intermediate reflux ratio*: a pinch in the middle of the column controls the separation. The composition x_N belongs to the linear approximation of column profile at x_B, whereas x_D is located in a binary axis of the more volatile components (or more generally in a distillation boundary).

(3) *High reflux ratio*: a pinch at the column top controls the separation with x_D being a pure component (or more generally an azeotrope).

Depending on the reflux ratio, batch rectifiers go through the three zones as rectification proceeds. Integration of Eqs. 6 and

7 is done until either a prefixed final recovery of a given species in the distillate or alternatively, a final rectification advance is achieved.

Operation at constant distillate composition requires calculating the minimum instantaneous reflux ratio $R_{\min}^{\text{inst}}$ to achieve a prefixed distillate composition for each still composition. The main characteristic of operation at constant distillate composition is that pinch points in the middle of the column control the separation. Figure 5 shows the linearization of a column profile and the mass balance corresponding to the minimum instantaneous reflux necessary to achieve the azeotropic composition in the distillate from a given bottom composition.

Other operating policies, such as multilevel reflux policies or combination of constant reflux policy with constant distillate composition policy, are easily handled by the conceptual model.

Even though integrating Eqs. 6 and 7 for a batch rectifier operating at constant distillate composition gives the variable reflux policy corresponding to minimum energy demand, the minimum reflux ratio necessary for a column operating at constant reflux ratio requires solving Eqs. 6 and 7 for several values of R until achieving prefixed recoveries of key components. The procedure is outlined elsewhere.[18]

Column performance at total reflux limiting operating condition is adequately described by solving a sequence of equilibrium and mass balance computations from a given still composition to predict the instantaneous distillate composition and assuming a differential rate of product withdrawal from the column at any time. The method used to attain the minimum number of stages is an iterative procedure where an initial guess of N is refined until the specified recovery fractions of two components are reached in the distillate. The simulations are stopped when the amount of the light-key component in the distillate corresponds to the specified component recovery, $\sigma_{LK,D.}$ Then, the amount of the heavy-key component in the distillate is used to drive the iteration on N until this amount corresponds to the specified fractional recovery, $\sigma_{HK,D}$.

The pseudo-homogeneous model is applied as a first approximation for the studied mixture, given that the adopted reflux policy corresponds to the one with the hetero-azeotrope returned as column reflux.[17] This means that both the CH-rich and W-rich phases, OP and AP in Figure 1, are refluxed to the column with an overall composition corresponding to that of the ternary azeotrope. It must be noted that in other systems it may be convenient to reflux only one phase from the settler.[20]

The interaction between both models

As already mentioned, the optimal feed composition should lie in the line connecting the ternary azeotrope with pure isopropanol. In this case, homogeneous azeotropic cuts do not show up and, thus, not only is maximum alcohol recovery achieved at the rectification end but the column operation is also optimized. Therefore, the optimization program involves only two pseudo-components in the distillation model to represent the main separation: the ternary azeotrope and pure isopropanol. The relative volatility between them is the parameter that must be estimated to run the optimization model.

The interaction between the optimization and the performance models is explained based on the main separation S_1. The same concepts apply for separation S_2. The idea is simple: a first guess for $\alpha_{\text{Azeo–IPA}}$ is proposed and the optimization model is solved. For each separation (in terms of component mole fraction and component recoveries) the predicted $R_{\min}$ is compared with the values calculated from the conceptual dynamic model. A refinement of the parameter $\alpha_{\text{Azeo–IPA}}$ is done until the deviation between the minimum reflux ratio of each separation task in both the optimization and the performance levels is acceptable.

Table 3 shows the optimization results for the main separation, consisting of three distillation tasks. The first guessed value for the parameter $\alpha_{\text{Azeo–IPA}}$ was 2 and, as can be seen, the reflux ratios predicted by the optimization level and the performance level disagree only slightly.

Figure 6 shows the multilevel reflux policy vs. the water composition in the still as the rectification proceeds, obtained at the optimization level. Figure 6 also shows the curve of minimum energy demand as obtained at the performance level. Because the still path lies in the line formed by the ternary azeotrope and pure isopropanol, the water mole fraction in the still completely defines the compositions of the remaining components. Thus, the instantaneous minimum reflux ratio necessary to achieve the composition of the ternary azeotrope at the column top can be calculated.

Figure 5 shows graphically the calculation of the minimum reflux ratio for an instantaneous still composition [0.18397 CH, 0.74421 IPA, 0.07182 W] from linearization of liquid profiles at the column bottom. Alternatively, the same result can be obtained by integrating Eq. 6 until a selected component recovery or rectification advance is achieved. At each value of the rectification advance, the minimum reflux ratio is estimated to reach the prefixed distillate composition.

From the curve of minimum energy demand it is clear that the separation becomes increasingly difficult as the composition in the still approaches the alcohol vertex in Figure 1b. The two first reflux levels are large enough to almost maintain the distillate composition at a constant value (ternary azeotropic composition) because the selected reflux policy is above the curve of minimum energy demand during the first two steps. During the last step, however, a variable distillate composition operation occurs until the final IPA bottom composition is achieved, and therefore an intersection between the reflux policy and the minimum energy demand curve takes place. It is clear that the curve of minimum instantaneous reflux acts as a limiting curve and thus it was incorporated into the optimization framework as a path constraint, which was represented by linear overestimators. Note that in Figure 6 the minimal trespassing of the minimum energy demand curve, which occurs at the first reflux level, arises from the linear approximation of this curve.

The curve of minimum energy demand can be also used to generate better first estimations of the parameter $\alpha_{\text{Azeo–IPA}}$ for the optimization program. For each still composition pertaining to the line formed by the ternary azeotrope and pure isopropanol, the corresponding composition of the pseudo-components can be calculated first and then the minimum reflux ratio needed to achieve the ternary azeotrope through the lever arm rule:

$$R_{\min}^{PseudoC\ Model} = \frac{(1 - Y_{\text{Azeo}})}{(Y_{\text{Azeo}} - X_{\text{Azeo}})} \tag{8}$$

Table 3. Optimization Results for S_1 Operating at Three Different Reflux Ratio Levels with $\alpha_{Azeo-IPA} = 2$*

		Amount (kmol)	Mole Fraction CH IPA Water	Reflux Ratio R Comp. Recov. σ Rectify. Adv η
S_{11}	F	58.8542	0.3145	R = 3.10
			0.5628	σ_W = 0.6337
			0.1227	σ_{IPA} = 0.1435
	D_{11}	21.0617	0.557	η = 0.3673
			0.2257	R_{min} 2/46/**2.06**
			0.2173	
	B_{11}	37.7925	0.1794	
			0.7506	
			0.0700	
S_{12}	D_{12}	6.5156	0.5573	R = 6.53
			0.2252	σ_W = 0.5273
			0.2175	σ_{IPA} = 0.051
	B_{12}	31.3780	0.10215	η = 0.1697
			0.8580	R_{min} 4.58/**4.80**
			0.03986	
S_{13}	D_{13}	8.0776	0.3887	R = 17.07
			0.4596	σ_W = 0.9795
			0.1517	σ_{IPA} = 0.1379
	B_{13}	23.3004	0.00280	η = 0.2574
			0.9961	R_{min} 15.29/**16.48**
			0.00109	

*Boldface values correspond to those calculated from the conceptual dynamic model.

Note that to calculate $R_{min}^{PseudoC\ Model}$ it is necessary to know the composition Y_{Azeo} that in turn depends on X_{Azeo} (known) and $\alpha_{Azeo-IPA}$ (unknown) through the equilibrium equation:

$$Y_{Azeo} = \frac{\alpha_{Azeo-IPA} X_{Azeo}}{1 + X_{Azeo}(\alpha_{Azeo-IPA} - 1)} \quad (9)$$

Therefore, a value for the parameter $\alpha_{Azeo-IPA}$ can be estimated to minimize the deviation between the conceptual model estimations, $R_{min}^{CBD\ Toolkit\ Model\ Model}$ and the pseudo-binary model predictions, $R_{min}^{PseudoC\ Model}$. Figure 7 shows quite good agreement between both model predictions if the feasible composition space is divided into three regions, giving rise to three values of $\alpha_{Azeo-IPA}$ [1.950, 1.884, 1.865].

Table 4 presents the overall results obtained by using the above values. A better approach than using a single value of the parameter is obtained by minimizing the sum of the squares of the differences between the predictions from the pseudo-binary model and the estimations from the dynamic conceptual model based in pinch analysis (Φ), which is lower than in the previous, arbitrary estimation of a unique relative volatility. Further refinement of relative volatilities could be done by redefining the region in which the composition space in Figure 7 is divided, from the results given by the optimization level.

Process Optimization Model

The model for process optimization, presented in this section, consists of a set of linear and nonlinear equations and inequations. A 120-h period make span is considered for processing 25 m^3 of IPA. Table 1 lists the feed, product, and working time specifications.

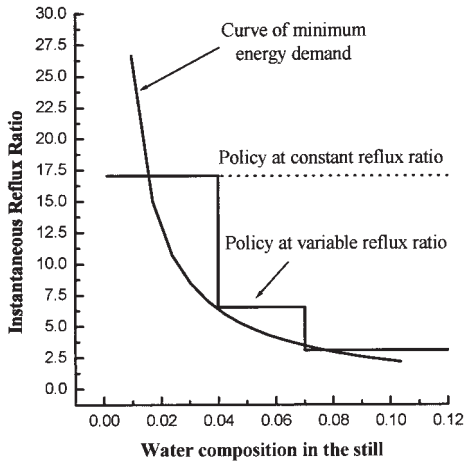

Figure 6. Minimum "instantaneous" reflux ratio to achieve the ternary azeotropic composition and multilevel reflux policy vs. water mole fraction in the still.

Decision variables

The optimization model handles the different consecutive distillation tasks performed by a single column. The amount of water-rich phase to be processed in a week is an unknown variable, as well as the composition of this mixture: they depend on how the first separation task was performed. Furthermore, the batch size, number of batches, and the processing time assigned to each batch are also unknown variables, that is, process decision variables.

Moreover, each separation task S_i can be performed by one or more subtasks k that will be conducted at different reflux ratios R_{ik} at the different consecutive processing times θ_{ik}. Separation S_1 is performed by distillation tasks S_{11}, S_{12}, and S_{13} and separation S_2 is carried out by just one distillation task, named simply S_2. The equipment involved in performing tasks

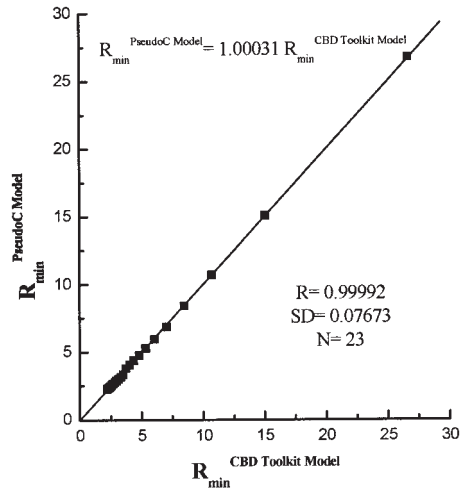

Figure 7. Correlation between values of R_{min} calculated from the performance model and the pseudo-binary model.

$\alpha_{Azeo-IPA}$ = [1.950, 1.884, 1.865].

S_1 and S_2 consists of a distillation vessel or still, an evaporator, a condenser, and the distillation column.

Each task and subtask will be performed sharing the same equipment; thus the design of all the equipment items should observe proper operability conditions. These conditions will be imposed by suitable constraints. For instance, the column diameter value will be constrained by the vapor velocity. In all tasks or subtasks the vapor velocity will be upper and lower bounded by suitable operative values. The optimal size of the batch and the optimal distillate composition for separation S_1 determines the amount of fresh feed processed and the amount of OP and AP exiting task S_1.

The mass balances presented in Table 2, which correspond to the states–tasks diagram of Figure 2 were computed such that the batch sizes involved in separation S_1 are the actual sizes, given that they result from the optimization program. As can be observed, the amount of AP reported in state 22 is an order of magnitude smaller than the figure that corresponds to, say, the fresh feed to S_1 (state 8). This amount of AP is actually a fraction of the optimal batch size for separation S_2, which will be of the same order of magnitude of S_1 to avoid underutilization of the facility. After a suitable number of batches for S_1 have been processed, the amounts of AP accumulated will be the next feed for separation S_2. The total available time in the week will be distributed between tasks S_1 and S_2. In this case study the optimal ratio was approximately 14:1.

The optimal operation cycle times of each batch result from a complex trade-off involving several components: equipment size for batch items (vessels), start-up and changeover times, size of continuous items (distillation column, evaporator and condenser), and operating costs. However, for practical reasons, these cycle times should be simple fractions of 8-h work shifts, such that the scheduling of tasks of one particular shift does not change every other day.

In this study case, the unconstrained optimal operating times were found to be a noninteger value about 7 h. Then, the optimization model was solved constraining them to be 4 or 8 h, from which was selected 8 h because this rendered a better value for the objective function. This in turn rounded the optimal distribution of the week make span between separations S_1 and S_2 to the fraction 14:1, that is, 14 of the total 15 available shifts of 8 h were assigned to separation S_1.

Operation Times. The time required by each separation S_i was modeled assuming the contributions of a variable processing time θ_i, a dead (fixed) time T_{fix_i}, and an equilibration time to reach the regimen conditions T_{reg_i}, which was computed by the heuristic rule of threefold the time required to vaporize the holdup of the distillation column, which is also a variable:

$$T_{reg_i} = 3\varepsilon(0.6N)A_{trnv}\rho_{mix_i}\frac{\Delta H_{vap}}{U_{evap}A_{evap}\Delta T_{evap}} \qquad \varepsilon = 0.1 \quad (10)$$

This equation derives from the energy balance in the evaporator. The volume of the column is $0.6NA_{trnv}$, where N is the number of separation stages; A_{trnv} is the cross-sectional area of the column; and ε is the fraction of column volume occupied with liquid.

If a separation S_i is performed at different reflux ratios R_{ik} the processing time θ_i is computed as

$$\theta_i = \sum_k \theta_{ik} \quad (11)$$

The total time in the week assigned to carry out separation S_i is represented by T_i, which is also an optimization variable. The sum of times T_i for all separations S_i is constrained by the operating time available in a week $T = 120$ h, and more than one batch can be produced in time T_i. Then

$$\theta_i + T_{fix_i} + T_{reg_i} \le T_i \quad (12)$$

$$\sum_i T_i = T \quad (13)$$

and the number of batches NB_i for S_i is computed by

$$NB_i = \frac{T_i}{\theta_i + T_{fix_i} + T_{reg_i}} \ge 1 \quad (14)$$

The number of batches to be processed in separation S_2 is related to the number of batches resulting from S_1 through the following relation between operation times:

$$\frac{NB_2}{NB_1} = \left(\frac{T_2}{T_1}\frac{\theta_1 + T_{fix_1} + T_{reg_1}}{\theta_2 + T_{fix_2} + T_{reg_2}}\right) \quad (15)$$

From practical and operative arguments, it is desirable that separations be performed in simple fractions of a working shift of 8 h, and thus the optimal solution was rounded as already mentioned.

Table 4. Optimization Results for the Main Separation S_1 Operating at Three Different Reflux Ratio Levels with $\alpha_{Azeo-IPA}$ = [1.950, 1.884, 1.865]*

		Amount (kmol)	Mole Fraction CH IPA Water	Reflux Ratio R Comp. Recov. σ Rectif. Adv. η
S_{11}	F	62.752	0.3146 0.5626 0.1228	R = 3.10 σ_W = 0.6346 σ = 0.1449
	D_{11}	22.532	0.5560 0.227 0.217	η = 0.3590 R_{min} 2.56/**2.02**
	B_{11}	40.221	0.1794 0.7506 0.070	
S_{12}	D_{12}	7.532	0.5559 0.2271 0.2169	R = 7.70 σ_W = 0.5803 σ_{IPA} = 0.0567
	B_{12}	32.688	0.09264 0.8712 0.03615	η = 0.1873 R_{min} 5.53/**5.06**
S_{13}	D_{13}	7.874	0.3758 0.4776 0.1466	R = 20.16 σ_W = 0.9770 σ_{IPA} = 0.1321
	B_{13}	24.814	0.0028 0.9961 0.00109	η = 0.2409 R_{min} 17.97/**17.15**

*Boldface values were calculated with the conceptual dynamic model. Φ = 1.1849.

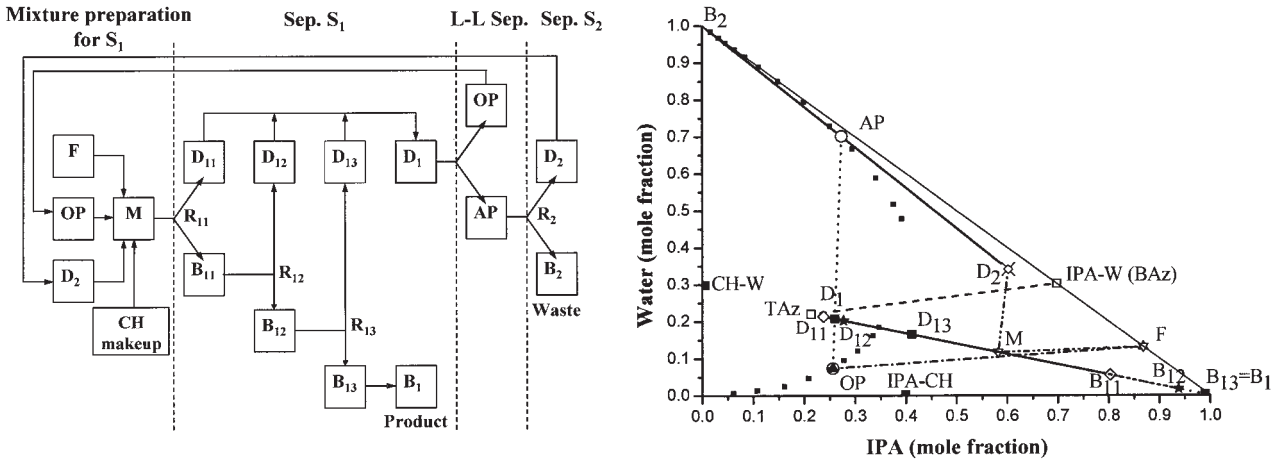

Figure 8. (a) Interconnection of tasks in the optimization model; (b) triangular diagram of the system showing the materials, mixtures, and compositions.

Volumes and Heat Transfer Areas. The volume of the distillation vessel V_{DV} and the areas of the evaporator A_{evap}, condenser A_{cond}, and of the distillation column A_{trnv} are decision variables. All these items must be large enough to perform any of the tasks assigned to both separations S_1 and S_2.

Reflux Ratios and Number of Stages of the Distillation Column. As mentioned, a separation task S_i can be performed by k distillation subtasks at different reflux ratios R_{ik}, which are decision variables to be optimized. The number of stages N of the distillation column also results from optimization.

Batch Sizes. The sizes of the batches to be processed are decision variables. The batch size of final product obtained by separation S_1 is calculated through

$$B_{batch\ 1} = W_{B1} + \mathrm{IPA}_{B1} + \mathrm{CH}_{B1} \tag{16}$$

where W_{B1}, IPA_{B1}, and CH_{B1} are the amounts of water, IPA, and CH remaining at the end of separation S_1 and, if P_{IPA} is the required production of IPA in the horizon time T, it must be verified that

$$P_{\mathrm{IPA}} = NB_1B_{batch\ 1} \tag{17}$$

Composition of the Mixtures to be Distilled. All the compositions x of the process mixtures, except the fresh feed, are subject to optimization. To clarify the materials, mixtures, and compositions involved, a scheme of the process model for optimization with the tasks is presented in Figure 8a, which coincides with the structure of the states–tasks diagram of Figure 2. Figure 8b presents the same information in a triangular diagram.

Objective function

A cost function based on the total annual cost (TAC)[21] is the objective function to be minimized. The investment and installation costs for process units, demand for steam, cooling water, entrainer reposition, and cost for wasting valuable product (IPA) in the effluent are considered. The objective function is of the type

$$-\Psi = \mathrm{TAC} = \mathrm{CCF}\left[\sum_j \alpha_j V_j^{\beta_j} + \sum_h \alpha_h Z_h^{\beta_h}\right] + \sum_m C_m M_m Q \tag{18}$$

where α_j, β_j, α_h, and β_h are the cost coefficients for the process units. The size of the batch and semicontinuous equipment are represented by V_j and Z_h, respectively. C_m represents the specific costs for utilities (steam and cooling water) and for the makeup of CH and IPA wasted. M_m represents the utility consumptions per unit of final product for an annual production rate Q. CCF is the capital charge factor, which is based on a 10-year amortization period and on 12.5% of the investments as annual maintenance cost. The cost coefficients and costs involved in the model are listed in Table 5.

Constraints

Distillation Model. The distillation model used for optimization is based on the simplified analytical model for binary distillations described in section III. The compositions and amounts of pure components must be converted into compositions and amounts of pseudo-components. The conversion of the pure components of the mixture M that enters to separation S_1 to pseudo-components in terms of molar amounts is expressed as

$$M_L = (\mathrm{W}_M + \mathrm{CH}_M) + (\mathrm{W}_M + \mathrm{CH}_M)\frac{x_{\mathrm{IPA}\ T_{\mathrm{Az}}}}{1 - x_{\mathrm{IPA}\ T_{\mathrm{Az}}}} \tag{19}$$

$$M_H = \mathrm{IPA}_M - (\mathrm{W}_M + \mathrm{CH}_M)\frac{x_{\mathrm{IPA}\ T_{\mathrm{Az}}}}{1 - x_{\mathrm{IPA}\ T_{\mathrm{Az}}}} \tag{20}$$

Conversely, the batches that exit a separation by distillation must be reconverted from pseudo-components to pure components. The distillates obtained by tasks S_{11}, S_{12}, and S_{13} for separation S_1 are mixed before the decantation task; that is

Table 5. Cost Functions, Coefficients, and Unitary Costs Used in the Model

Item	Cost	Units
	Investment Plus Installation Costs	
Condenser	$3627.5A^{0.65}$	A (m^2)
Evaporator	$4895A^{0.65}$	A (m^2)
Horiz. vessel	$3111V^{0.6}$	V (m^3)
Distillation column	$32635(0.6N)^{0.65}A_T^{0.65} + 4860 \times 0.6NA_T$	N: N° stages A_T (m^2)
	Utility Costs	
Steam vapor	5.5×10^{-3}	U$D/kg
Cooling water	8×10^{-2}	U$D/$m^3$
	Cost for Material Wasted in the Effluent	
IPA	457	U$D/$m^3$
Cyclohexane	256	U$D/$m^3$

$$D_{L_i} = \sum_k D_{L_{ik}} \qquad D_{H_i} = \sum_k D_{H_{ik}} \tag{21}$$

Liquid–Liquid Separation Model. The envelope and the two phases coexisting region of the liquid–liquid equilibrium for the IPA–cyclohexane–water system is approximated by linear inequalities:

- Organic phase

$$\begin{aligned} x_{\text{IPA OP}} &\le 0.91679 - 0.91824x_{\text{CH OP}} \\ x_{\text{IPA OP}} &\le 0.68388 - 0.63828x_{\text{CH OP}} \\ x_{\text{IPA OP}} &\le 0.51067 - 0.35x_{\text{CH OP}} \\ x_{\text{IPA OP}} &\le 0.4545 - 0.2298x_{\text{CH OP}} \end{aligned} \tag{22}$$

- Aqueous phase

$$\begin{aligned} x_{\text{IPA AP}} &\le 0.3784 + 0.09822x_{\text{CH AP}} \\ x_{\text{IPA AP}} &\le 0.3040 + 0.6657x_{\text{CH AP}} \\ x_{\text{IPA AP}} &\le 0.1681 + 4.058x_{\text{CH AP}} \\ x_{\text{IPA AP}} &\le 0.00106 + 109.63x_{\text{CH AP}} \end{aligned} \tag{23}$$

The tie lines joining the corresponding experimental data pairs are approximated by nonlinear equations:

$$x_{\text{IPA OP}} = x_{\text{IPA AP}} + (0.17958 - 0.754x_{\text{IPA AP}})(x_{\text{CH OP}} - x_{\text{CH AP}}) \tag{24}$$

The experimental data of the liquid–liquid equilibrium for the IPA–W–CH system,[22] the envelope approximating functions, and a few approximated tie lines are plotted in Figure 9.

Maximum Feasible Distillate Composition for S_2. The maximum feasible distillate composition in separation S_2 is constrained by the distillation boundary joining the binary azeotrope IPA–W and the ternary azeotrope IPA–CH–W, which is linearly approximated through the following equation:

$$\frac{x_{\text{IPA } D_2} - x_{\text{IPA } T_{\text{Az}}}}{x_{\text{IPA } B_{\text{Az}}} - x_{\text{IPA } T_{\text{Az}}}} \le \frac{x_{\text{W } D_2} - x_{\text{W } T_{\text{Az}}}}{x_{\text{W } B_{\text{Az}}} - x_{\text{W } T_{\text{Az}}}} \tag{25}$$

Path Constraints. The curve of minimum energy demand for separation S_1 is approximated by linear constraints as shown in Figure 10. As explained in section II, the two first distillation tasks for S_1 are conducted at reflux ratios such that the distillate produced is almost pure CH–IPA–W. Thus, the reflux ratios for distillation tasks S_{11} and S_{12} have to satisfy the following constraints:

$$\begin{aligned} R_{1k} &\ge 5.3194 - 31.70577x_{\text{W } B_{1k}} \qquad k = 1, 2 \\ R_{1k} &\ge 10.98667 - 112.66667x_{\text{W } B_{1k}} \qquad k = 1, 2 \\ R_{1k} &\ge 19.52 - 326x_{\text{W } B_{1k}} \qquad k = 1, 2 \end{aligned} \tag{26}$$

Purity. The purity specifications and permitted limits reported in Table 1 on the bottom products for separations S_1 and S_2 are imposed through the constraints:

$$\begin{aligned} x_{\text{W } B_1} &\le x^{\text{lim}}_{\text{W}_{B_1}} \\ x_{\text{CH } B_1} &\le x^{\text{lim}}_{\text{CH}_{B_1}} \end{aligned}$$

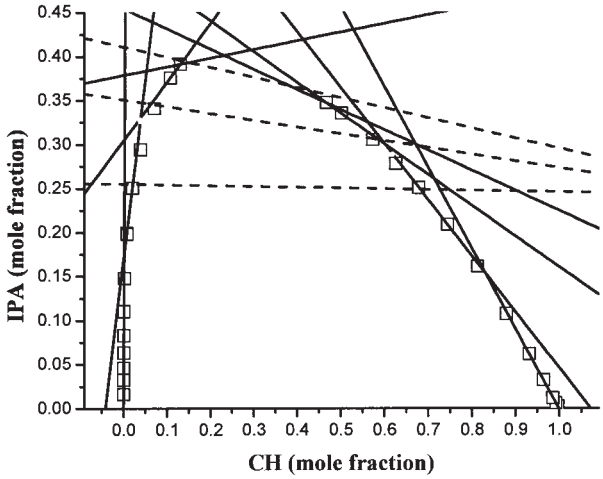

Figure 9. Experimental data (square symbols), envelope approximating functions (solid lines), and a few tie lines (dash lines).

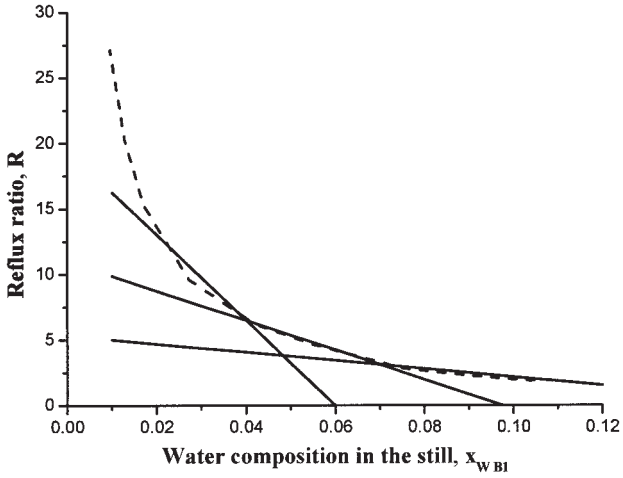

Figure 10. Approximation of the minimum energy demand curve for separation S_1.

$$x_{\mathrm{IPA}\,B_1} \geq x^{\lim}_{\mathrm{IPA}_{B_1}}$$
$$\mathrm{IPA}_{B_2} \leq \frac{\mathrm{W}_{B_2}\mathrm{PM}_{\mathrm{W}} + \mathrm{CH}_{B_2}\mathrm{PM}_{\mathrm{CH}} + \mathrm{IPA}_{B_2}\mathrm{PM}_{\mathrm{IPA}}}{\rho_{\mathrm{W}}} \frac{10^{-6}\mathrm{IPA}^{\lim}_{B_2}}{\mathrm{PM}_{\mathrm{IPA}}} \tag{27}$$

Mass Balances. The mass balances are computed on a S_1 batch size basis. Preparation of the mixture M to be processed in a batch of separation S_1:

$$\begin{aligned} \mathrm{IPA}_M &= \mathrm{IPA}_F + \mathrm{IPA}_{\mathrm{OP}} + \mathrm{IPA}_{D_2} \\ \mathrm{W}_M &= \mathrm{W}_F + \mathrm{W}_{\mathrm{OP}} + \mathrm{W}_{D_2} \\ \mathrm{CH}_M &= \mathrm{CH}_{makeup} + \mathrm{CH}_{\mathrm{OP}} + \mathrm{IPA}_{D_2} \end{aligned} \tag{28}$$

In these equations, IPA_F and W_F as well as the other variables are unknown amounts to be processed or obtained in one batch of separation S_1 and will be determined by optimization.

- Balance for the separation S_1

$$\begin{aligned} \mathrm{IPA}_M &= \mathrm{IPA}_{D_1} + \mathrm{IPA}_{B_1} \\ \mathrm{W}_M &= \mathrm{W}_{D_1} + \mathrm{W}_{B_1} \\ \mathrm{CH}_M &= \mathrm{CH}_{D_1} + \mathrm{CH}_{B_1} \end{aligned} \tag{29}$$

- Balance for the liquid–liquid separation (*LLS*)

$$\begin{aligned} \mathrm{IPA}_{D_1} &= \mathrm{IPA}_{\mathrm{OP}} + \mathrm{IPA}_{\mathrm{AP}} \\ \mathrm{W}_{D_1} &= \mathrm{W}_{\mathrm{OP}} + \mathrm{W}_{\mathrm{AP}} \\ \mathrm{CH}_{D_1} &= \mathrm{CH}_{\mathrm{OP}} + \mathrm{CH}_{\mathrm{AP}} \end{aligned} \tag{30}$$

- Balance for the separation S_2

$$\begin{aligned} \mathrm{IPA}_{\mathrm{AP}} &= \mathrm{IPA}_{D_2} + \mathrm{IPA}_{B_2} \\ \mathrm{W}_{\mathrm{AP}} &= \mathrm{W}_{D_2} + \mathrm{W}_{B_2} \\ \mathrm{CH}_{\mathrm{AP}} &= \mathrm{CH}_{D_2} + \mathrm{CH}_{B_2} \end{aligned} \tag{31}$$

Note that all the variables in the equations for separation S_2 also refer to the amounts of the components involved in one batch of separation S_1.

Design. Note that the following design equations are written as "greater than or equal to" inequalities. The optimization will drive some of the inequalities to equalities. The material amounts to be processed are related to the mass balance amounts computed for one batch of separation S_1.

- Volume of the distillation vessel V_{DV} for separation S_1

$$V_{DV_1} \geq \frac{M_{L_1} + M_{H_1}}{\rho_{mix_1}} \tag{32}$$

- Evaporator area for separation S_{1k}, A_{evap_1}

$$A_{evap1} \geq \frac{\Delta H_{vap_1}}{U_{evap}\Delta T_{evap}} \frac{(R_{1k}+1)(D_{L_{1k}} + D_{H_{1k}})}{\theta_{1k}} \qquad k = 1, 2, 3 \tag{33}$$

- Condenser area for separation S_{1k}, A_{cond_1}

$$A_{cond_1} \geq \frac{\Delta H_{cond_1}}{U_{cond}\Delta T_{cond}} \frac{(R_{1k}+1)(D_{L_{1k}} + D_{H_{1k}})}{\theta_{1k}} \qquad k = 1, 2, 3 \tag{34}$$

- Area of the distillation column for separation S_{1k}, A_{trnv_1}

$$A_{trnv1} \geq \frac{1}{\rho_{V_1} v_{V_1} 3600} \frac{(R_{1k}+1)(D_{L_{1k}} + D_{H_{1k}})}{\theta_{1k}} \qquad k = 1, 2, 3 \tag{35}$$

Note that the batch size for separation S_2 corresponds to the amount of AP obtained in one batch of separation S_1 ($M_{L_2} + M_{H_2}$) times the number of batches of S_1 and divided by the number of batches of S_2 in a week.

- Volume of the distillation vessel V_{DV} for separation S_2

$$V_{DV_2} \geq \frac{M_{L_2} + M_{H_2}}{\rho_{mix2}} \left(\frac{T_1}{T_2} \frac{\theta_2 + T_{fix_2} + T_{reg_2}}{\theta_1 + T_{fix_1} + T_{reg_1}} \right) \tag{36}$$

- Evaporator area for separation S_2, A_{evap_2}

$$A_{evap2} \geq \left[\frac{\Delta H_{vap_2}}{U_{evap_2}\Delta T_{evap_2}} (R_2 + 1) \right] \times \frac{D_{L_2} + D_{H_2}}{\theta_2} \left(\frac{T_1}{T_2} \frac{\theta_2 + T_{fix_2} + T_{reg_2}}{\theta_1 + T_{fix_1} + T_{reg_1}} \right) \tag{37}$$

- Condenser area for separation S_2, A_{cond_2}

Table 6. Model Parameter Values and Input Data

Parameter	Value		Units
	Sep. 1	Sep. 2	
α_{LH}	2.0/2.0/2.0 $S_{11}/S_{12}/S_{13}$	10.0	—
ρ_{mix}	12	34	kmol/m^3
$\rho_{B_{Az}}$		15.2	kmol/m^3
$\rho_{T_{Az}}$	12		kmol/m^3
U_{evap}	1452.78	1627.11	W m^{-2} K^{-1}
U_{cond}	784.5		W m^{-2} K^{-1}
ΔT_{evap}	25	25	K
ΔT_{cond}	25	40	K
ΔH_{vap}	37.49	41.66	kJ/kmol
ρ_V	0.035		kmol/m^3
v_V	1.15	1.25	m/s
λ_{H_2O}	2.448		kJ/kg
C_p	4.184		kJ m^{-3} K^{-1}
ΔT_{H_2O}	20		K

$$A_{cond_2} \geq \left[\frac{\Delta H_{vap_2}}{U_{cond_2}\Delta T_{cond_2}}(R_2+1)\right] \times \frac{D_{L_2}+D_{H_2}}{\theta_2}\left(\frac{T_1}{T_2}\frac{\theta_2+T_{fix_2}+T_{reg_2}}{\theta_1+T_{fix_1}+T_{reg_1}}\right) \quad (38)$$

- Area of the distillation column for separation S_2, A_{trnv_2}

$$A_{trnv_2} \geq \left[\frac{1}{\rho_{V_2} v_{V_2} 3600}(R_2+1)\right] \times \frac{D_{L_2}+D_{H_2}}{\theta_2}\left(\frac{T_1}{T_2}\frac{\theta_2+T_{fix_2}+T_{reg_2}}{\theta_1+T_{fix_1}+T_{reg_1}}\right) \quad (39)$$

Because all the separation tasks are carried out in a unique distillation column, the following constraints have to be satisfied:

$$\begin{aligned} N_1 - N_2 &= 0 \\ V_{DV_1} - V_{DV_2} &= 0 \\ A_{evap_1} - A_{evap_2} &= 0 \\ A_{cond_1} - A_{cond_2} &= 0 \\ A_{col_1} - A_{col_2} &= 0 \end{aligned} \quad (40)$$

Model parameters and data

Table 6 lists the model parameter values and input data.

Statistics and computational aspects

The *nonlinear programming* (NLP) model was implemented in the *general algebraic modeling system* (GAMS)[23] and solved using the CONOPT solver,[24] which is based on a reduced-gradient algorithm. The model statistics are presented in Table 7. The optimization model is solved in less than 1 s of total CPU time. The total time for problem setup and execution needed by CBD Toolkit to calculate minimum reflux is around 45 s of wall clock time for each distillation task. So, <4 min are needed to perform one iteration between both models.

Results and Discussion

The optimal design corresponding to the model parameter values and input data listed in Tables 1 and 6 is presented through the reports of the equipment sizes in Table 8, of the operating times in Figure 4, and costs in Table 9. A dead (fixed) time of 35 min was assigned to both separations S_1 and S_2.

A sensitivity analysis was performed based on a local sensitivity method that computes the local gradients of the objective function, the total annual cost, with respect to infinitesimal parameter variations. Specifically, the analysis is focused on the relative marginal values (RMV) for each model parameter p_i investigated:

$$\mathrm{RMV}_i = \frac{\partial \Psi}{\partial p_i}\frac{p_i}{\Psi} \quad (41)$$

Changes in the model parameters such as feed composition, production specifications, dead (fixed) times, cost factors, distillation model parameters, and effluent limits are investigated. Generally, large changes in the optimal solution for small changes in the model parameters are not desirable. Table 10 ranks the parameters based on the descendent absolute values of the relative marginals (RMAVs).

The sign of the relative marginals indicates the direction of the change on the objective function. As it is here defined, a positive relative marginal implies an increase in the total annual cost when increasing the parameter value.

The analysis of the parameters investigated identifies parameters critical for the plant design and operation and model parameters involved in physicochemical and cost calculations and effluent permitted limits. Among the former, the largest RMAV corresponds to the mole fraction of IPA in the fresh feed x_{IPA_F}. The production rate P_{IPA} and the maximum vapor velocity in the distillation column for separation v_{V_1} exhibit the second and third largest values, respectively. The RMAV for the dead time for separation S_1 (T_{fix_1}) is one order of magnitude higher compared to that of separation S_2. An increase in the dead time T_{fix_1} requires larger batch sizes and, consequently, larger volumes. However, the heat transfer areas and the cross-sectional area of the distillation column are almost insensitive because the times to perform separation tasks θ_i are instead increased to satisfy the production rate stipulated. This result is not evident from the RMA values but from the sensitivity of process variables to finite (arbitrary) perturbations on the model parameters.

The relative volatility $\alpha_{LH_{13}}$ to carry out separation task S_{13} has a strong impact in the total annual cost. By increasing $\alpha_{LH_{13}}$ a significant reduction in the total annual cost is predicted because the reflux ratio for this task is, indeed, high (15.29). Savings can be obtained by assigning different relative volatile values to the different distillation tasks involved in separation

Table 7. Optimization Model Statistics

Optimization Model Statistics			
Blocks of equations:	196	Single equations:	190
Blocks of variables:	164	Single variables:	164
Nonzero elements:	653	Nonlinear N-Z:	342
Derivative pool:	39	Constant pool:	44
Code length:	3999		

Table 8. Equipment Sizes

Equipment	Charact. Dimension	Value	Utility	Value (max)
Distillate cooler	Area (m^2)	4.85	Water (m^3/h)	0.73
Product cooler	Area (m^2)	2.57	Water (m^3/h)	0.4236
Condenser 1	Area (m^2)	19.58	Water (m^3/h)	17.85
Condenser 2	Area (m^2)	4.8	Water (m^3/h)	4.234
Boiler	Area (m^2)	11.51	Steam (kg/h)	804
Column			Amount	
Sectional area	Area (m^2)	0.267		
Diameter	Diam. (m)	0.583		
Height	Min. theor. stages	13		
Still	Vol (m^3)	5	2	
IPA Preprocessing			Utility	Value (Max)
Evap-crystallizer	Diam (m)	0.54	Steam (kg/h)	98.44
	Vol. (m^3)	0.186		
Partial condenser	Diam. (m)	0.181	Water m^3/h	0.4
	Length (m)	0.53		
Condenser-cooler	Area (m^2)	3.23	Water (m^3/h)	1.9241
Storage tanks			Amount	
Clean IPA tank	Vol. (m^3)	2	2	
OP tank	Vol. (m^3)	6.5	2	
AP tank	Vol. (m^3)	4.2	1	

S_1, as described in the main body of the paper. Because the vaporization heat ΔH_{vap_1} involved in separation S_1 is generally estimated with acceptable certainty, its influence on the final design is minimized.

Among the cost model coefficients, the capital charge factor (CCF) exhibits the largest RMAV. The cost of steam α_6 is the most influential one of the operation costs. The factor α_{5a}, which is related to the cross-sectional area of the distillation column, has the largest impact on the equipment investment costs. This is also reflected by the high RMAV for the vapor velocity v_{V_1} as noted above, which has an inverse relation to the column cross-sectional area. This area is dominated by separation S_1 because the vapor velocity for separation S_2 (v_{V_2}) exhibits a zero RMAV.

With respect to the effluent permitted limits, the objective function is sensitive to the allowable loss of cyclohexane in the effluent from S_1 ($x^{lim}_{\mathrm{CH}\,B_1}$) but insensitive to water ($x^{lim}_{\mathrm{W}\,B_1}$), whose RMAV is zero. The impact of the limit imposed to IPA for separation S_2 is one order of magnitude lower compared to that of cyclohexane for S_1. The objective function is almost insensitive to the IPA cost C_{IPA} but sensitive to cyclohexane C_{CH}, whose RMAV is two orders of magnitude higher than the former.

The RMAVs for the global heat transfer coefficient U_{cond_2} and the temperature differences ΔT_{cond_2} for the condenser of the distillation column to perform separation S_2 are zero, given that the design of the cooling system is dominated by the requirements for separation S_1. Moreover, the design of the whole plant is governed by separation S_1. This is concluded based on the higher RMAVs for parameters involved in separation S_1 compared to S_2 such as U_{cond}, ΔT_{cond}, U_{evap}, ΔT_{evap}, T_{fix}, ΔH, v_V, and α_{LH}.

Table 9. Cost Results

Cost Items	Value
Total annual cost (TAC) (U$D/a)	5.5133×10^4
Purchased equip. cost FOB (U$D)	5.3743×10^4
Purchased + Installation (U$D)	1.2323×10^5
Annual operation costs (U$D/a)	2.7407×10^4
Cost of Individual Units—FOB (U$D)	
Distillation still	3.6714×10^3
Evaporator	9.2507×10^3
Condenser	1.1014×10^4
Distillation column	1.7231×10^4
Parking	9.8619×10^3
Total investment cost	5.3743×10^4
Investment plus installation (U$D)	
Distillation still	8.0771×10^3
Evaporator	2.1739×10^4
Condenser	2.5884×10^4
Distillation column	5.1694×10^4
Total	1.2323×10^5
Operation costs (U$D/a)	
Steam	1.8281×10^4
Cooling water	7.7778×10^3
Makeup of CH	1.3186×10^3
IPA lost in residue	2.9469

Table 10. Sensitivity Analysis

	Parameter	RMV
x_{IPA_F}	IPA mole fraction in fresh feed F	−2.343
$\alpha_{LH_{13}}$	Relative volatility for S_{13}	−0.893
P_{IPA}	IPA production	0.835
ΔH_{vap_1}	Vaporization heat for S_1	0.552
CCF	Capital charge factor	0.503
$\lambda_{\mathrm{H_2O}}$	Water vaporization latent heat	−0.331
α_6	Cost of steam	0.331
α_{5a}	Cost coef. for distillation column	0.211
β_4	Cost exponent for condenser	0.208
$\alpha_{LH_{11}}$	Relative volatility for S_{11}	−0.196
v_{V_1}	Vap. linear vel. in column for S_1	−0.187
$\Delta T_{\mathrm{H_2O}}$	Cooling water temp. difference	−0.141
α_7	Cost of cooling water	0.141
β_3	Cost exponent for evaporator	0.132
$x^{lim}_{\mathrm{CH}_B1}$	Limit mole fraction of CH in B_1	−0.124
α_4	Cost coefficient for condenser	0.105
β_5	Cost exponent for distil. column	0.097
α_3	Cost coefficient for evaporator	0.088
$\alpha_{LH_{12}}$	Relative volatility for S_{12}	−0.077
U_{cond_1}	Cond. heawt transfer coef. for S_1	−0.06866
ΔT_{cond_1}	Cond. temp. difference for S_1	−0.06866
ΔH_{vap2}	Vaporization heat for S_2	0.0466
α_{LH_2}	Rel. volatility for separation S_2	−0.0464
α_{5b}	Cost coef. for column packing	0.0402
U_{evap_1}	Evap. heat transfer coef. for S_1	−0.0385
ΔT_{evap_1}	Evap. temp. difference for S_1	−0.0385
α_1	Cost coef. for distillation vessel	0.0329
β_1	Cost exponent for distil. vessel	0.03145
C_{CH}	Cost of cyclohexane	0.02391
T_{fix_1}	Dead time assigned to S_1	0.02303
U_{evap_2}	Evap. heat transfer coef. for S_2	−0.01944
ΔT_{evap_2}	Evap. temp. difference for S_2	−0.01944
$\mathrm{IPA}^{lim}_{B_2}$	Max. permit conc. of IPA in B_2	−0.00901
T_{fix_2}	Dead time assigned to S_2	0.00194
C_{IPA}	Cost of IPA	0.00053
$X^{lim}_{\mathrm{W}_B1}$	Limit mole fraction of H_2O in B_1	0
v_{V_2}	Vap. linear vel. in column for S_2	0
U_{cond_2}	Cond. heat transfer coef. for S_2	0
ΔT_{cond_2}	Cond. temp. difference for S_2	0

Conclusions

Two distillation models with different degrees of detail were integrated to achieve the optimal design of an industrial distillation facility. These models are a conceptual dynamic model that accounts for the vapor–liquid nonideality of the multicomponent system, and a process optimization model that resorts to a simplified binary Fenske–Underwood–Gilliland-type model.

Although the distillation models have already been published, the novel contributions of this paper are the interaction between both, and the process optimization model that practically implements highly nonlinear constraints and models real operation features as the merging of small batches before reprocessing and the rounding of optimal processing times to yield simple operation schedules.

The highly nonlinear constraints are posed by the liquid–liquid separation and the operation policy of switching to higher reflux ratios when the minimum energy demand curve is approached.

The merging of the small aqueous phase batches was done without further complicating the nested system of equations that represent the mass balances, but adding constraints that distribute the weekly makes pan between the IPA and aqueous phase separations. Furthermore, this distribution of operation times was rounded to attain distillation cycles compatible with 8-h shifts.

Although this process optimization program permits optimizing the batch sizes, number of separation stages, the piecewise constant reflux operation policy, and the size of the intermediate cuts to be recycled, it resorts to a simplified unit operation model. So, the conceptual dynamic model that accounts for nonideality of the multicomponent system is used from outside the optimization program both to verify feasibility of the design and to update the parameters of the simplified model.

The criterion used for this integration was to achieve coincidence of both models in their predictions of the minimum reflux needed by each separation, that is, the energy demands of each task handled by the process optimization program are validated by the conceptual model. The interaction between models could be initialized with arbitrary values for the relative volatilities among pseudo-components, but a better first estimation was proposed through minimization of the deviation between the models' predictions of the minimum reflux ratios.

The interaction between both models allowed us to solve a complete optimization program (yet relying on a simplified physical model), still accounting for the highly nonlinear liquid–vapor and liquid–liquid equilibrium of the system, with affordable computational and problem setup times.

Use of the binary FUG model for this three-component system was valid under the specific operation policy dictated by the previous conceptual design analysis. In a general azeotropic batch distillation one might have to resort to more detailed models.

Acknowledgments

The financial support from Consejo Nacional de Investigaciones Científicas y Técnicas (CONICET) and Agencia Nacional de Promoción Científica y Tecnológica (ANPCyT), and permission for publishing the industrial design by Materias Primas Medicinales MAPRIMED S.A. of Argentina are gratefully acknowledged.

Notation

A = heat transfer area, m^2
A_{trnv} = cross-sectional area of the distillation column, m^2
AP = aqueous phase cut from the decantation step (refers to water-rich phase)
B_1 = refers to the still content at the end of separation S_1
B_2 = refers to waste-water cut of separation S_2
B_{batch_1} = batch size of final product obtained by separation S_1, kmol
CBD = conceptual batch distillation
CCF = capital charge factor
CH = amount of cyclohexane, kmol
CH–IPA–W = ternary hetero-azeotrope
CH–W, CH–IPA, IPA–W = binary azeotropes
C_m = specific cost for utility m (U$D/kg vapor, U$D/m^3 cooling water)
C_p = cooling water specific heat capacity, kJ m^{-3} K^{-1}
D = amount of distillate, kmol
D_1 = overall amount of distillate collected after separation task S_1 is completed, kmol
D_2 = refers to distillate cut of separation S_2
F = amount of fresh feed to the process, kmol
IPA = amount of isopropyl alcohol, kmol
M = mixture to be distilled
M_{H_i} = amount of the heavy key pseudo-component in mixture to be distilled by separation task S_i, kmol
M_{L_i} = amount of the light-key pseudo-component in mixture to be distilled by separation task S_i, kmol
M_m = consumption of utility m per unit of final product for an annual production rate Q
N = actual number of separation stages
N_{min} = minimum number of stages for a total reflux batch column
NB_i = number of batches corresponding to separation S_i
OP = organic phase cut from the decantation step (refers to cyclohexane-rich phase)
P_{IPA} = required production of IPA in the horizon time T, kmol
PM = molecular weight, g/mol
Q = annual production rate
R = actual reflux ratio
R_{min} = minimum reflux ratio for a batch column with infinite number of trays
S_i = separation task i
T = operation time available in a week (120 h)
T_{fix_i} = dead (fixed) time for separation task S_i, h
T_{reg_i} = equilibration time to reach the regimen conditions for separation task S_i, h]
T_i = total time in the week assigned to carry out separation S_i, h
TAC = total annual cost, U$S
U = global heat transfer coefficient, W m^{-2} K^{-1}
V = unit process volume, m^3
V_j = size of the batch equipment
v_V = vapor linear velocity in the distillation column, m/s
W = amount of water, kmol
x = composition in mole fraction
x_B = instantaneous still composition
x_D = instantaneous distillate composition
x_{iD} = mole fraction of component i in the distillate
x_{i0} = initial mole fraction of component i in the still
x_{LI} = intermediate mole fraction value of the light-key component in the still
x_N = composition of the liquid stream in the stage immediately above the reboiler
$y^*_{x_B}$ = mole fraction of the vapor phase in equilibrium with the still content of composition x_B
X_{Azeo} = mole fraction of the ternary azeotrope (pseudo-component) in liquid phase
Y_{Azeo} = mole fraction of the ternary azeotrope (pseudo-component) in vapor phase
Z_h = size of the semicontinuous equipment

Greek letters

σ_{iD} = fractional recovery of component i in the distillate
η = rectification advance
$\sigma_{LK,D}$ = specified fractional recovery of the light-key component in the distillate
$\sigma_{HK,D}$ = specified fractional recovery of the heavy-key component in the distillate
$\alpha_{Azeo-IPA}$ = relative volatility between the ternary azeotrope and isopropanol
Φ = sum of the squares of the differences between the predictions from pseudo-binary model and dynamic conceptual model based in pinch theory
θ_{ik} = processing time to perform task k of separation task S_i, h
ε = volume fraction of the distillation column occupied with liquid
ρ_{mix} = density of the mixture to be distilled, kmol/m^3
ρ = density, kmol/m^3
ΔH = vaporization heat, kJ/kmol
ΔT = temperature difference, K
Ψ = objective function; (= $-$TAC)
$\alpha_{j,\ \beta j,\ \alpha h,\ \beta h}$ = cost coefficients for the process units
ρ_V = water vapor density, kmol/m^3
λ_{H2O} = water vaporization latent heat, kJ/kg

Subscripts

B_i = bottom material obtained at the end of separation task S_i
B_{ik} = bottom material obtained by (sub)task k of separation task S_i
B_{Az} = binary azeotrope
CH = refers to cyclohexane
cond = condenser
D_i = distillate obtained at the end of separation S_i
D_{ik} = distillate obtained by (sub)task k of separation S_i
DV = distillation vessel
evap = evaporator
F = fresh feed
i = separation (distillation) task
H = heavy-key component (or pseudo-component)
IPA = isopropyl alcohol
k = step (subtask) of a separation task S_i
L = light-key component (or pseudo-component)
M = mixture M
mix = mixture to be distilled
trnv = cross-sectional area
TAz = ternary azeotrope
V = vapor
vap = vaporization
W = water

Superscripts

CBD = conceptual batch distillation
D = distillate
lim = purity permitted limit
0 = initial

Literature Cited

1. Bernot C, Doherty MF, Malone MF. Feasibility and separation sequencing in multicomponent batch distillation. *Chem Eng Sci.* 1991; 46:1311-1326.
2. Ahmad BS, Barton PI. Solvent recovery targeting. *AIChE J.* 1999;45: 335-349.
3. Safrit BT, Westerberg AW. Synthesis of azeotropic batch distillation separation systems. *Ind Eng Chem Res.* 1997;36:1841-1854.
4. Rodriguez-Donis I, Gerbaud V, Joulia X. Feasibility of heterogeneous batch distillation processes. *AIChE J.* 2002;48:1168-1178.
5. Chiotti OJ, Iribarren OA. An optimization module for batch distillation with intermediate cuts. *Comput Ind.* 1989;13:169-180.
6. Chiotti OJ, Salomone HE, Iribarren OA. Selection of multicomponent batch distillation sequences. *Chem Eng Commun.* 1993;119:1-21.
7. Bernot C, Doherty MF, Malone MF. Design and operating targets for non-ideal multicomponent batch distillation. *Ind Eng Chem Res.* 1993; 32:293-301.
8. Sundaram S, Evans LB. Synthesis of separations by batch distillation. *Ind Eng Chem Res.* 1993;32:500-510.
9. Noda M, Kato A, Chida T, Hasebe S, Hashimoto I. Optimal structure and on-line optimal operation of batch distillation column. *Comp Chem Eng.* 2001;25:109-117.
10. Skouras S, Skogestad S. Separation of ternary heteroazeotropic mixtures in a closed multivessel batch distillation–decanter hybrid. *Chem Eng Process.* 2004;43:291-304.
11. Kondili E, Pantelides CC, Sargent RWH. A general algorithm for short term scheduling of batch operations. *Comp Chem Eng.* 1993;17:211-227.
12. Mujtaba IM, Macchietto S. Optimal operation of multicomponent batch distillation—Multiperiod formulation and solution. *Comput Chem Eng.* 1993;17:1191-1207.
13. Mujtaba IM, Macchietto S. Simultaneous optimization of design and operation of multicomponent batch distillation column—Single and multiple separation duties. *J Process Contr.* 1996;6:27-36.
14. Bhatia T, Biegler LT. Dynamic optimization in the design and scheduling of multiproduct batch plants. *Ind Eng Chem Res.* 1996;35:2234-2246.
15. Logsdon JS, Diwekar UM, Biegler LT. On the simultaneous optimal design and operation of batch distillation columns. *Trans IChemE.* 1990;68(Part A):434.
16. Espinosa J, Salomone E. Minimum reflux for batch distillations of ideal and non-ideal mixtures at constant reflux. *Ind Eng Chem Res.* 1999;38:2732-2746.
17. Espinosa J, Salomone E, Iribarren O. Computer-aided conceptual design of batch distillation systems. *Ind Eng Chem Res.* 2004;42:1723-1733.
18. Salomone HE, Chiotti OJ, Iribarren OA. Short cut design procedure for batch distillations. *Ind Eng Chem Res.* 1997;36:130-136.
19. Bauerle GL, Sandall OC. Batch distillations of binary mixtures at minimum reflux. *AIChE J.* 1987;33:1034-1036.
20. Rodriguez-Donis I, Pardillo-Fontdevila E, Gerbaud V, Joulia X. Synthesis, experiments and simulation of heterogeneous batch distillation processes. *Comput Chem Eng.* 2001;4/6:799-806.
21. Douglas JM. *Conceptual Design of Chemical Processes*. New York, NY: McGraw-Hill; 1988.
22. Verhoeye LAJ. The system cyclohexane-2-propanol-water. *J Chem Eng Data.* 1968;13:462-467.
23. Brooke A, Kendrick D, Meeraus A. *GAMS: A User's Guide*. Release 2.25. South San Francisco, CA: The Scientific Press; 1992.
24. Drud AS. *CONOPT: A System for Large Scale Non-linear Optimization* (Reference manual for CONOPT subroutine library). Bagsværd, Denmark: ARKI Consulting and Development A/S; 1996.

Manuscript received Aug. 6, 2004, revision received Jun. 8, 2005, and final revision received Aug. 25, 2005.